# ANALYSIS OF LATERAL FUEL MIXING IN A FLUID-DYNAMICALLY DOWN-SCALED BUBBLING FLUIDIZED BED

Erik Sette[a]*, Sonia Aimé[b], David Pallarès[a], Filip Johnsson[a]

[a] Chalmers University of Technology; Dept. Energy and Environment, SE-41296 Göteborg, Sweden
[b] INSA de Lyon; Dept. Energy and Environment, 69621 Villeurbanne Cedex, France
*T : 0046 31 772 1446; E : sette@chalmers.se

## ABSTRACT

A method to evaluate the lateral mixing process of fuel particles in bubbling fluidized beds is proposed. The method determines the lateral dispersion coefficient of the fuel particles by means of digital image analysis to video recordings of tracer particle measurements in a fluid-dynamically downscaled 3-dimensional cold-flow model. The work applies direct measurements of tracer particles coated with fluorescent paint, which are irradiated with an ultraviolet light emitting lamp, mounted above the bed. The cold-flow model has cross-sectional dimensions of 0.3 m x 0.3 m and can be operated with bed heights up to 0.16 m. According to the scaling laws this setup is assumed to fluid-dynamically resemble a bubbling fluidized bed operated at 900°C with cross-sectional dimensions of 1.5 m x 1.5 m and bed heights up to 0.8 m. The measurements were made for fluidization velocities ranging from 0.17 to 0.83 m/s (up-scaled).

The lateral fuel dispersion coefficient is found to increase with superficial velocity over the entire range of velocities investigated. The results show up-scaled (i.e. at hot conditions) dispersion coefficients ranging from $10^{-2}$ to $10^{-1}$ $m^2/s$, which is similar to values obtained previously in large-scale bubbling beds under hot conditions.

## INTRODUCTION

The phenomenon of mixing is of great importance in most large-scale chemical processes, such as combustion and gasification. Mixing promotes mass and heat transfer which are crucial factors in the process of converting fuel in fluidized bed combustion and gasification reactors. The lateral mixing of fuel is a key parameter in fluidized bed boilers. Sufficiently fast mixing is required in order to ensure complete burn out of fuel (1) and to minimize the number of fuel feeding ports (2). For fluidized bed indirect gasifiers (also known as allothermal gasifiers) which are connected to a boiler in order to generate the heat needed for the endothermic gasification reactions (3), the lateral fuel mixing has to be controlled. The lateral fuel mixing has to be kept at a moderate level to give the fuel sufficient time to be converted by the gasification reactions (which are slower than the combustion reactions (4)). Thus, increased fuel mixing yields increased loss of char from the gasifier to the connected boiler, where it is combusted (3). Fluidized bed boilers and gasifiers of commercial

scale have large cross-sectional bed area and are operated with a low bed aspect ratio (height to width ratio of the dense bed) (5). Partly as a consequence of this, mixing in the vertical direction is faster than in the lateral direction (6). Thus, in boilers, lateral mixing is the limiting factor in the overall fuel mixing, which implies a risk for uneven fuel distribution resulting in oxygen-depleted zones with incomplete burn out as well as zones with an excess of oxygen. In particular, release of volatile matter can become relatively concentrated in the vicinity of fuel feeding ports, increasing the risk for incomplete volatile combustion in the furnace.

In summary, there is a need to investigate and develop modeling tools which can describe the fuel mixing process under conditions relevant for industrial scale combustors and indirect gasifiers. This work is a step in this direction and has the aim to establish a method which can quantify the lateral mixing of fuel particles in a bubbling fluidized bed by combining experiments with mathematical modeling. The method is used to investigate the influence of superficial gas velocity on the lateral fuel dispersion. The experimental work is conducted in a fluid-dynamically downscaled cold-flow model of a large-scale bubbling fluidized bed.

Literature proposes three main solids mixing mechanisms for the solids in fluidized beds under bubbling conditions (7, 8): 1) the solid particles are pulled upwards by the wake behind rising bubbles, 2) particles flow downwards with the emulsion phase around bubbles and 3) particles are scattered over the dense bed surface when a bubble erupts. Since these mechanisms are all goverened by the bubble flow they are of an intermittent nature and the resulting solids flow can be seen as convective. However, it is common to lump the effects together and describe the overall mixing behavior with one diffusion like equation in which a so-called dispersion coefficient (accounting for both diffusive and convective transport) is used, which applied to the two horizontal dimensions reads:

$$\frac{\partial C}{\partial t} = \frac{\partial C}{\partial x} D_x \cdot \left( \frac{\partial C}{\partial x} \right) + \frac{\partial C}{\partial y} D_y \cdot \left( \frac{\partial C}{\partial y} \right) \tag{1}$$

Furthermore, for an even distribution of the primary gas nozzles over the gas distributor cross section, it is common to assume that the dispersion coefficients are equal in both horizontal directions, *i.e.* $D_x = D_y = D$.

The dispersion coefficient in Eq. 1 can be evaluated from experimental data according to Einstein's equation for brownian motion (9).

$$D = \frac{(\Delta L)^2}{2\Delta t} \tag{2}$$

Where *L* is the distance travelled by the particle during the time period *t*.

A review of findings from previous works on fuel mixing (10, 11) reveals large differences in experimental values of lateral fuel dispersion coefficients, spaning over several orders of magnitude, even for cases applying similar operational conditions.

## EXPERIMENTAL SETUP

A fluid-dynamically downscaled cold-flow model was used in the experiments (Fig. 1, left). The unit has a square cross-section of 0.3 m x 0.3 m. The bed height is variable up to 0.16 m but was kept at 0.11 m during the tests reported in the present work. Sanderson and Rhodes (12) have showed that fluid-dynamic scaling is important in order to achieve similarity between two bubbling fluidized beds. Thus, the unit is downscaled according to Glicksman's scaling laws (13) with a length scaling factor of 5 and resembles a unit of cross-sectional dimensions of 1.5 m x 1.5 m and bed height of 0.55 m, which is operated at 900 °C. The paricle diameter is scaled by keeping the particle Reynold's number constant between the two units. The minumum fluidization velocity for the cold-flow model is 0.010 m/s, which corresponds to an upscaled velocity of 0.022 m/s. The cold-flow model is equipped with an orifice plate, with uniform spacing between the orifices in both lateral directions. Throughout all experiments presented in this work, the same orifice plate was used. In order to simplify the conditions, a high pressure drop air distributor was chosen with a pressure drop higher than what is typical for industrial large-scale units. Future work will investigate the influence of air distributor pressure drop and allocation of the orifices.

This work applies superficial velocities from 0.07 m/s to 0.37 m/s in the cold-flow model, i.e. corresponding to 0.17 m/s - 0.83 m/s when scaled up. All other operating conditions are kept constant.

a.

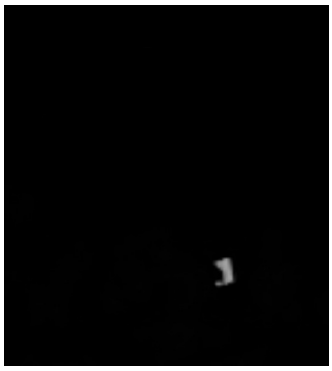

b.

Figure 1: (a) The experimental unit used. The ultraviolet light lamp is visible at the upper left corner. The camera used for video recordings is located next to the UV-lamp. (b) Colored tracer particle (black-and white photo here) viewed from above glows brightly which enables detection of its position.

In order to simplify the detection, this work applies a single fuel tracer particle, although the method allows for simultaneous tracking of several particles by means of color

detection. The shape, size and density of the tracer particle used are chosen as to be representative for a wood chip under full scale conditions. As a result from the scaling laws, bronze powder was used as bed material and polystyrene as tracer particle. A detailed description of the scaling of the bed material in the current system is given in (14). As seen in Table 1 the density ratio between the fuel particle and the bed material is kept approximately constant between the large scale unit and the cold flow model, i.e. this should result in dynamic similarity between the two units. However, since exact matching of the density ratio was not possible (the density of the tracer particle is 14 % lower than required), the tracer particle can be expected to have a slightly higher flotsam tendency.

It must be noted that fluid-dynamic downscaling is not able to capture any effects of physical or chemical changes in the fuel particle. A real fuel particle releases moisture and volatiles during conversion. This rapid release of gases is believed to increase the floatsam behavior of the fuel particle (15). However, the time scale for drying and devolatilization should be much smaller than that for char conversion, suggesting that any enhancement in floatsam behavior due to gas release is only important for a short time of the in-bed residence time of the fuel particle.

Table 1: Summary of parameters in the large scale and downscaled beds

| Parameter | Unit | Large scale | Downscaled |
|---|---|---|---|
| Bed dimension (Length x Width) | m | 1.5 x 1.5 | 0.3 x 0.3 |
| Density, bed material | $kg/m^3$ | 2600 | 8900 |
| Density, fuel | $kg/m^3$ | 400 | 1200 |
| Density ratio (bed material / fuel) | - | 6.5 | 7.4 |
| Temperature | ℃ | 900 | 20 |
| Length scale factor | m | L | L/5 |
| Superficial velocity | m/s | u | $\sqrt{\frac{u^2}{5}}$ |

As indicated above, this work applies direct measurements of one tracer particle coated with fluorescent paint. The tracer particle is injected by gravity (dropped down) to the center of the bed at the beginning of an experiment. While the bed is being fluidized, the ultraviolet light emitting lamp, *i.e.* a black light, mounted above the bed (Fig. 1a) makes the tracer particle glow brightly. Due to the high contrast between the colored particle and the surrounding environment, which appears black, it is possible to track the particle, Fig. 1b. The motion of the fuel particle is recorded with a digital video camera, recording at a rate of 25 frames per second, followed by digital image analysis to quantify the dispersion of the tracer particle. This analysis applies an algorithm for the detection of the colored region of a video frame in order to determine the position of the tracer (fuel) particle. Having the particle position over time, the dispersion of the fuel particles is estimated by Eq. (2).

The particle can obviously only be tracked once it emerges at the surface and is not covered by splashing bed material. Thus, there can be a considerable number of frames in-between two detections. Therefore there is a risk that the particle hits a wall while submerged in the bed, thus distorting the analysis. In order to exclude this wall effect, the observations which are estimated to have happened after the tracer particle has hit a wall while being immersed in the bed must be removed in the analysis. Figure 2 compares a valid tracer particle location (Fig. 2a) with one for which the data point has to be excluded from analysis (Fig. 2b). The surrounding circle indicates the distance which the tracer particle is expected to travel during the time it is immersed in the bed. This distance is calculated according to the Einstein's equation (Eq. 2) as the square-root of two times the lateral dispersion coefficient times the time the particle is immersed in bed. Thus the lateral dispersion coefficient is required to determine this distance. The radius of the circle varies with fluidization velocity since it depends on the lateral dispersion coefficient. In Fig.2a, the tracer particle is not expected to hit any wall in the given time between particle detections, thus this data point is kept in the calculation of the dispersion coefficient. In Fig. 2b, the particle could have hit the wall while immersed in the bed (the circle intersects with the boundary of the bed), i.e. this data point is removed from the calculation of the dispersion coefficient. An iterative procedure is applied in order to update the lateral dispersion coefficient and to determine which detections to remove since they depend on each other.

a. b.

Figure 2: Location of the tracer particle before immersion (dot) and expected traveled distance after immersion time (circle). a): valid data point for the analysis. b): discarded data point in the analysis

## RESULTS AND DISCUSSION

Figure 3 presents results from the fuel dispersion experiments. The dispersion coefficient is calculated for both lateral directions (*x* and *y*) and is found to increase with gas velocity (Fig. 3a). The dispersion coefficients in the *x* and *y* directions are consistently close to each other, although not exactly matching. The deviation in the two directions from the average value is displayed in Fig. 3b. The deviation in both *x* and *y* directions appears to be normal distributed and the deviation from zero is approximately equal in both directions. Thus the difference in dispersion rate in the *x* and *y* directions is assumed to be random and not systematic, suggesting that the dispersion rate is equal in both horizontal directions.

Figure 4 shows the lateral dispersion coefficient averaged over the two lateral directions, including both the experimental values in the cold-flow model and the corresponding up-scaled values for the large scale unit. The trend is that increasing gas velocity yields higher lateral dispersion rate. However, as can be seen in Fig. 4 the increase in lateral dispersion coefficient with increased velocity for the range investigated is not constant, but a rather steeper slope is observed at higher fluidization velocities. The reason for this should be that the different mixing mechanisms varies with gas velocity, with the contribution from splashing at the surface caused by bubble eruptions on the lateral solids mixing increasing at higher gas velocities.

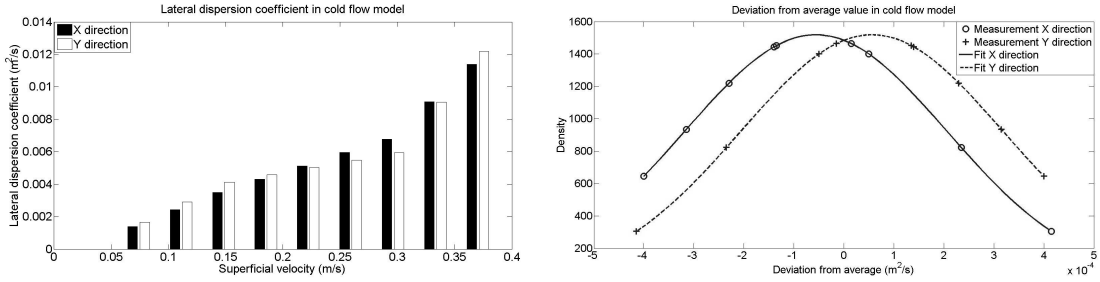


a. b.

Figure 3: (a) Lateral fuel dispersion coefficient obtained in cold flow model, for both *x* and *y* directions. (b) Deviation of the dispersion coefficient values from the average value, for both *x* and *y* direction.

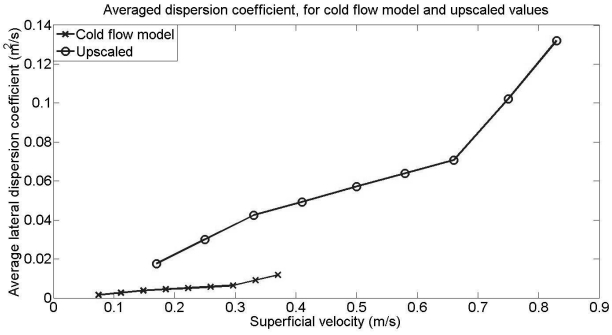


Figure 4: Lateral tracer dispersion coefficient as a function of superficial velocity, for experimental values obtained in the cold flow model and the corresponding up-scaled values.

The order of magnitude for the up-scaled lateral dispersion coefficients is in the range $10^{-2}$ to $10^{-1}$ $m^2/s$. This range can be compared with the value obtained by Niklasson et al. (11) of $10^{-1}$ $m^2/s$ for soaked wood chips by means of indirect measurements in a large scale fluidized bed (2.36 $m^2$ cross section) operating under hot conditions (900°C) at a fluidization velocity of 2.3 m/s and with a bed height of 0.5 m. Thus, this value is similar to the values of this work, although at considerably lower fluidization velocities (around 0.75 m/s, on up-scaled basis). There are two possible reasons for this difference: a) the downscaled fuel particles used have a lower density than that given by the scaling laws in order to resemble wood chips and b) the wood chips used in (11) were soaked in water, yielding a higher density than that of regular wood chips. The more flotsam tracer applied in the present work should enhance the lateral dispersion with an increase in velocity, as bubble eruptions take over as the main mixing mechanism. On the other hand, the present results disagree with the dispersion coefficients in the range $[0.46\text{-}0.68]*10^{-3}$ $m^2/s$ obtained by Olsson et al. (10) in a large-scale fluidized bed (1.44 $m^2$ cross section) operated with a fluidization velocity of 0.15 m/s and a bed height of 0.4 m at cold conditions, i.e. these experiments were not scaled. Thus, it is experimentally shown that, unless dynamic scaling is employed, the magnitudes of inter-particle and gas-particle forces governing the solids mixing differ between hot and cold conditions.

## CONCLUSIONS

A method for characterizing the lateral fuel mixing by means of digital image analysis has been developed and applied to a fluid dynamically down-scaled fluidized bed operated under ambient conditions. The method yields the same values for the dispersion coefficient in both lateral directions when using a gas distributor with uniform orifice spacing.

The lateral fuel dispersion coefficient is found to increase with superficial gas velocity. At high fluidization velocities, the mixing mechanism of splashing by bubble eruptions dominates, although this mechanism may be overestimated by the fact that the

downscaled fuel particle used in this work has a somewhat lower density than required by the scaling laws.

Compared to results obtained in large-scale units, the up-scaled results of the present work agree with previous data obtained under hot conditions, but not with data from cold large-scale runs which were not scaled.

## REFERENCES


1) D. Pallarès, P. A. Díez, F. Johnsson. (2007). Experimental analysis of fuel mixing patterns in a fluidized bed. *The 12th International Conference on Fluidization*, (ss. 929-936). Vancouver, Canada.

2) J. Highley, D. Merrick. (1971). Effect of the spacing between solid feed points on the perfomance of a large fluidized bed reactor. *AIChE Symposium Series 67*, 219-227.

3) H. Thunman, M. C. Seeman. (2009). First experience with the new Chalmers gasifier. *20th International Conference on Fluidized Bed Combustion*, (ss. 559-663). Xian.

4) A. Gómez-Barea, B. Leckner. (2010). Modeling of biomass gasification in fluidized bed. *Progress in Energy and Combustion Science 36*, 444-509.

5) T. Knoebig, K. Luecke, J. Werther. (1999). Mixing and reaction in the circulating fluidized bed - A three-dimensional combustor model. *Chemical Engineering Science 54*, 2151-2160.

6) O. Ito, R. Kawabe, T. Miyamoto, H. Orita, M. Mizumoto, H. Miyadera. (1999). Direct Measurment of Particle Motion in a Large-Scale FBC Boiler Model. *Fluidized Bed Combustion* (s. 0023). Savannah, Georgia: ASME.

7) D. Kunii, O. Levenspiel. (1991). *Fluidization Engineering.* Butterworth-Heinemann.

8) P. N. Rowe, B. A. Partridge, A. Cheney, G. Henwood, E. Lyall. (1965). The mechanisms of solids mixing in fluidized beds. *Transactions of the Insitution of Chemical Engineers, 43*, ss. 271-286.

9) A. Einstein. (1978). Investigations on the theory of the Brownian movement.

10) J. Olsson, D. Pallarès, F. Johnsson. (2012). Lateral fuel dispersion in a large-scale bubbling fluidized bed. *Chem. Eng. Sci. 74*, 148-159.

11) F. Niklasson, H. Thunman, F. Johnsson, B. Leckner. (2002). Estimation of Solids Mixing in a Fluidized-Bed Combustor. *Ind. Eng. Chem. 41*, ss. 4663-4673.

12) J. Sanderson, M. Rhodes. (September 2003). Hydrodynamic Similarity of Solids Motion and Mixing in Bubbling Fluidized Beds. *AIChE Journal, No 9, Vol 49*, ss. 2317-2327.

13) L. R. Glicksman, M. R. Hyre, P. A. Farrell. (1994). Dynamic Similarity in Fluidization. *Int. J. Multiphase Flow 20*, 331-386.

14) E. Sette, A. Gómez-García, D. Pallarès, F. Johnsson. (2012). Quantitative Evaluation of Inert Solids Mixing in a Bubbling Fluidized Bed. *Fluidized Bed Combustion*, (ss. 573-580). Neaples.

15) R. Solimene, A. Marzocchella, P. Salatino. (2003). Hydrodynamic interaction between a coarse gas-emitting particle and a gas fluidized bed of finer solids. *Powder Technology 133*, 79-90.